

Regulation of endodermal differentiation of human embryonic stem cells through integrin-ECM interactions

DA Brafman^{*1}, C Phung¹, N Kumar² and K Willert^{*1}

Many cellular responses during development are regulated by interactions between integrin receptors and extracellular matrix proteins (ECMPs). Although the majority of recent studies in human embryonic stem cell (hESC) differentiation have focused on the role of growth factors, such as FGF, TGF β , and WNT, relatively little is known about the role of ECMP-integrin signaling in this process. Moreover, current strategies to direct hESC differentiation into various lineages are inefficient and have yet to produce functionally mature cells *in vitro*. This suggests that additional factors, such as ECMPs, are required for the efficient differentiation of hESCs. Using a high-throughput multifactorial cellular array technology, we investigated the effect of hundreds of ECMP combinations and concentrations on differentiation of several hPSC lines to definitive endoderm (DE), an early embryonic cell population fated to give rise to internal organs such as the lung, liver, pancreas, stomach, and intestine. From this screen we identified fibronectin (FN) and vitronectin (VTN) as ECMP components that promoted DE differentiation. Analysis of integrin expression revealed that differentiation toward DE led to an increase in FN-binding integrin $\alpha 5$ (ITGA5) and VTN-binding integrin αV (ITGAV). Conditional short hairpin RNA-mediated knockdown of ITGA5 and ITGAV disrupted hESC differentiation toward DE. Finally, fluorescence-based cell sorting for ITGA5 and ITGAV significantly enriched cells with gene expression signatures associated with DE, demonstrating that these cell surface proteins permit isolation and enrichment of DE from hESCs. These data provide evidence that FN and VTN promote endoderm differentiation of hESCs through interaction with ITGA5 and ITGAV, and that ECMP-integrin interactions are required for hESC differentiation into functionally mature cells.

Cell Death and Differentiation (2013) 20, 369–381; doi:10.1038/cdd.2012.138; published online 16 November 2012

Human embryonic stem cells (hESCs), with their ability to differentiate into mature cell types, represent a novel system to study human development and disease, and assess safety and efficacy of drugs before clinical trials. In addition, these cells provide an unlimited source of 'raw material' for regenerative medicine therapies of many incurable diseases, including diabetes and heart disease. However, applications of hESCs in basic research, pharmaceutical, and regenerative medicine are hampered by the lack of well-defined conditions for their directed differentiation and insufficient methods for the purification of lineage-specific cell types from heterogeneous cell populations. Cells derived from definitive endoderm (DE), including those comprising the gut, lung, and pancreas, are of significant interest for many regenerative medicine purposes. Previous studies have identified conditions to generate DE from hESCs through growth factor or small molecule modulation of various soluble signaling pathways including TGF β , Wnt and AKT/PI3K.^{1–4} However, most DE differentiation protocols yield heterogeneous cell populations,⁴ suggesting that additional factors, such as

extracellular matrix proteins (ECMPs), are required for the specification of hESCs to specific fates.

While many studies have focused on the roles of signaling molecules in the differentiation of hESCs, relatively little is known about the role of ECMPs and their interactions with integrins in controlling hESC fate. In mammals, 24 heterodimeric integrin receptors consisting of one of 18 α -subunits and one of 8 β -subunits have been identified. In addition to mediating binding to specific ECMPs, which provide a scaffold for cell growth,^{5,6} activation of integrins through interactions with local ECMPs influence cellular processes during embryonic development, including cell survival, proliferation, motility and differentiation. Furthermore, the bidirectional (i.e. inside-out and outside-in) nature of integrin signaling serves as a link between the extracellular and intracellular environments and in turn modulates various downstream signaling pathways and components, such as MEK-ERK, PI3-kinase, and SRC.⁷ Moreover, many of these downstream pathways have previously been implicated in regulating hESC self-renewal, proliferation, and differentiation.⁷

¹Department of Cellular and Molecular Medicine, Stem Cell Program, University of California, La Jolla, CA, USA and ²Department of Bioengineering, University of California, La Jolla, CA, USA

*Corresponding authors: D Brafman or K Willert, Department of Cellular and Molecular Medicine, Stem Cell Program, University of California, UCSD, 9500 Gilman Drive, La Jolla, CA 92093-0695, USA. Tel: + 858 822 3235; Fax: + 858 246 1579; E-mail: dbrafman@ucsd.edu or kwillert@ucsd.edu

Keywords: human embryonic stem cells; arrayed cellular microenvironments; extracellular matrix proteins; integrin signaling; endoderm development

Abbreviations: Acta, Actinin A; COL I, collagen I; COL III, collagen III; COL IV, collagen IV; COL V, collagen V; DE, definitive endoderm; DOX, doxycycline; ECM, extracellular matrix; ECMP, extracellular matrix protein; FN, fibronectin; hESC, human embryonic stem cell; IF, immunofluorescence; ITGA5, integrin $\alpha 5$; ITGAV, integrin αV ; LN, laminin; MGEL, Matrigel; MMP, metalloproteinase; PE, pancreatic endoderm; PF, posterior foregut; PGT, primitive gut tube; qPCR, quantitative reverse transcription PCR; shRNA, short hairpin RNA; VTN, vitronectin; W3A, Wnt3a

Received 29.3.12; revised 21.8.12; accepted 2.10.12; Edited by R De Maria; published online 16.11.12

Therefore, the study of ECMP-integrin signaling is important in understanding the mechanisms that control hESC differentiation.

Current endodermal differentiation strategies involve guiding hESCs through sequential, staged protocols that mimic early embryonic signaling events known to control primitive streak formation and gastrulation. However, these protocols are often variable and inefficient, yielding only 30–40% cells expressing endodermal markers, such as SOX17. A potential strategy for improving hESC differentiation efficiency involves a two-pronged approach in which hESCs are differentiated to DE and then isolated and enriched using cell surface markers. This strategy not only relies on developing methods for improving the efficiency of DE differentiation from hESCs but also on methods for isolating endodermal cells from heterogeneous differentiating hESC cultures.

The majority of hESC differentiation protocols utilize poorly defined matrices, such as Matrigel (MGEL, BD Biosciences, San Jose, CA, USA), which is a protein mixture produced by EHS mouse sarcoma cells. While such protein extracts provide extracellular components necessary to support cell adhesion, they fail to mimic the specialized microenvironments to which cells are exposed *in vivo*. In this study, we employed a high-throughput combinatorial ECMP array platform to identify fibronectin (FN) and vitronectin (VTN) as components that improve differentiation of hESCs to DE. Furthermore, we show that the integrin receptors that engage FN and VTN are required for hESC differentiation to DE. Finally, we identified a novel DE integrin ‘signature’ that allows for fluorescence-based cell sorting methods to purify endodermal progeny from differentiating hESC cultures. Thus, our studies demonstrate the utility of investigating ECMP-integrin interactions to improve of hESC differentiation.

Results

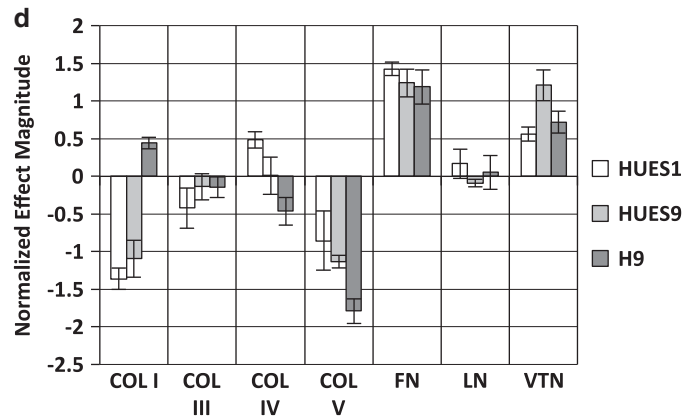
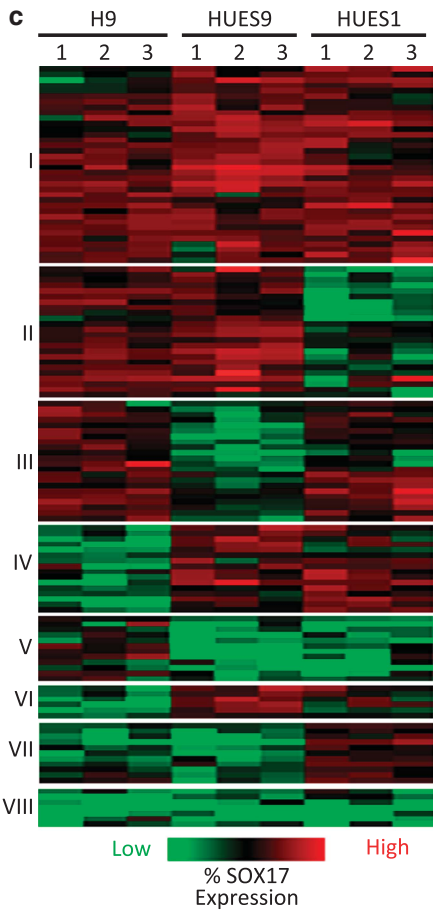
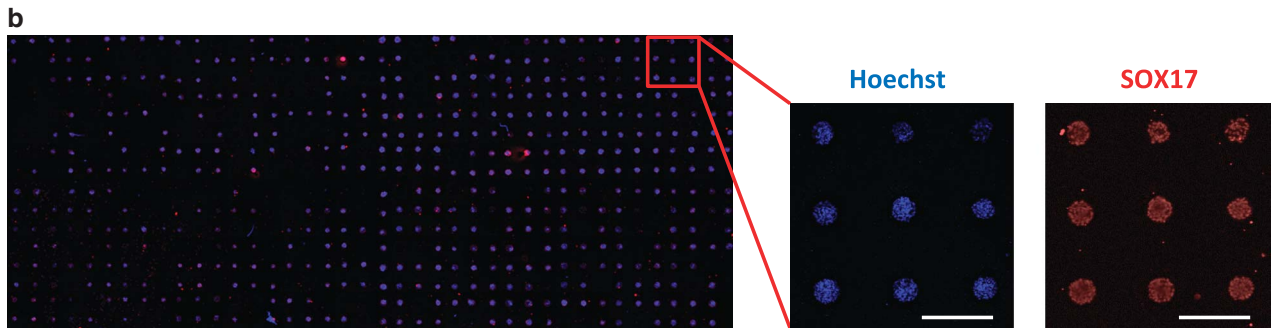
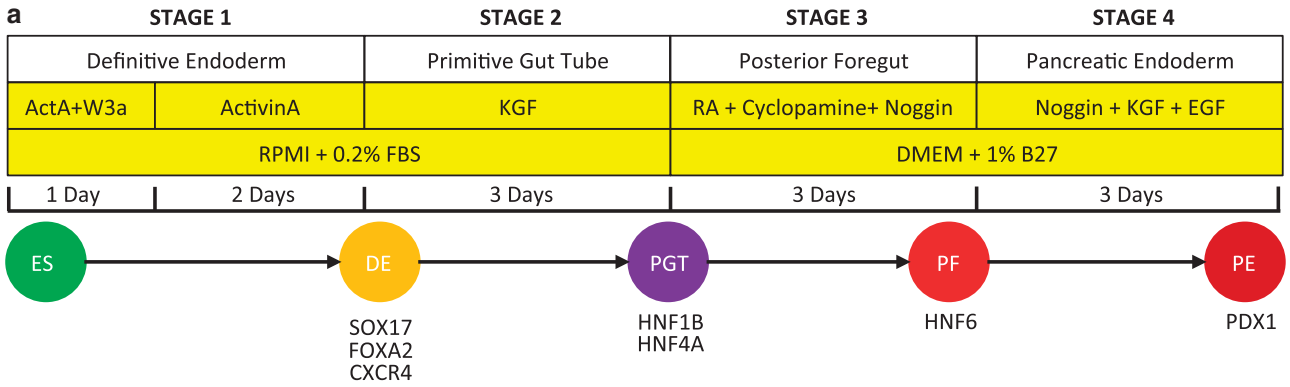
High-throughput cellular microarray screen to identify matrix components that promote endodermal differentiation. In an effort to further define and optimize current differentiation protocols of hESCs, we chose to examine the staged differentiation protocol toward pancreatic endoderm (PE, Figure 1a), the first stage of which involves Wnt3a and Activin A treatment to differentiate hESCs to DE,^{2,8,9} as assessed by expression of SOX17, FOXA2, and CXCR4. Although certain hESC lines, such as CyT49, efficiently differentiate into DE,^{2,8,9} other cell lines yield variable amounts of cells expressing DE marker genes, ranging from 32–65% (Supplementary Figure 1), suggesting that additional factors are required for DE differentiation. We sought to investigate to what extent the extracellular milieu, specifically ECMPs, affects endodermal differentiation of three hESC

lines, H9, HUES1, and HUES9. We employed a cellular microarray screening platform previously developed in our laboratory.^{10–13} All possible combinations of seven ECMPs, collagen I (COL I), collagen III (COL III), collagen IV (COL IV), collagen V (COL V), FN, laminin (LN) and VTN were printed on arrays as described (see Materials and Methods). For comparison we included MGEL (BD Biosciences), which is commonly employed in differentiation protocols of adherent hESC cultures. These arrays were seeded with hESCs, the medium was supplemented with Wnt3a and Activin A to promote endodermal differentiation, and cells were fixed, stained, and imaged for the DE marker SOX17 and DNA (Hoechst Stain 33342) (Figure 1b).

Hierarchical clustering of data sets revealed eight well-defined clusters (Figure 1c; for raw data see Supplementary Table 1), representing ECMP combinations that either promoted high normalized SOX17 expression in all three hESC lines tested (Cluster I), two out of three hESC lines tested (clusters II, III, and IV), one out of the three hESC lines tested (cluster V, VI, VII), or in none of the hESC lines tested (cluster VIII). Analysis of the Pearson correlation coefficient between independent array experiments demonstrated the consistent effects of ECMP combinations within each hESC line but also revealed that the efficiency of some ECMP conditions in promoting DE differentiation was cell line-specific (Supplementary Figures 2a and b). To identify the ECMPs that most effectively promoted DE formation, we performed a full factorial analysis,¹⁴ which revealed FN and VTN as the most common DE promoting ECMPs (Figure 1d). Other ECMPs had either no effect (e.g. LN) or negative effects (e.g. COL V) on DE differentiation (Figure 1d).

FN and VTN promote endodermal differentiation. To confirm that FN and VTN promoted DE differentiation of hESCs we compared their effects to that of MGEL in conventional cell culture formats. HUES9 hESCs were plated on MGEL and the combination of FN and VTN (FN + VTN) and differentiated to DE. Immunofluorescent (IF) staining demonstrated that FN + VTN caused a statistically significant increase in the percentage of cells expressing the DE marker SOX17 (Figure 2a). Moreover, culture on FN + VTN increased the total number of SOX17+ cells, as well as the total cell number (Figure 2b). Flow cytometry revealed that culture on FN + VTN produced an increase in the percentage of cells expressing the DE marker CXCR4 (Figure 2c). Finally, quantitative PCR (qPCR; Figure 2d) of DE markers *SOX17*, *FOXA2*, and *CXCR4* showed that FN + VTN increased the efficiency of DE differentiation relative to MGEL. We also observed that FN + VTN resulted in increased DE differentiation in two additional hESC lines, HUES1 and H9 (Supplementary Figures 3a and b). Finally, our analysis revealed that FN + VTN increased the efficiency

Figure 1 High-throughput ECMP screen reveals the influence of ECMPs in DE differentiation. (a) Schematic of the four stage differentiation protocol from hESC (ES), to DE, PGT, posterior PF, and finally PE. The soluble factors and culture media used at each stage are shown. (b) hESCs (H9, HUES1, HUES9) were cultured on ECMP arrays using previously published DE differentiation conditions.⁸ On day 3, arrays were fixed and stained with Hoechst and an antibody to SOX17, a marker for DE (scale bar = 450 μ m). (c) Heat map representing the cell number normalized SOX17 expression of each ECMP combination (rows) for each independent array experiment. Three independent array experiments were performed with each hESC line. Columns were mean normalized and scaled to one unit S.D. Hierarchical clustering of ECMP conditions was performed using Pearson correlation coefficient as a similarity metric. Clustering segregated ECMP combinations into eight groups based on the normalized SOX17 expression induced in each hESC line. (d) Magnitude of the main effects from a full factorial analysis of the ECMP array data reveals that specific ECMP components, FN and VTN, have largest positive effects on DE differentiation efficiency ($n = 3$ independent array experiments; error bars, S.E.M.)



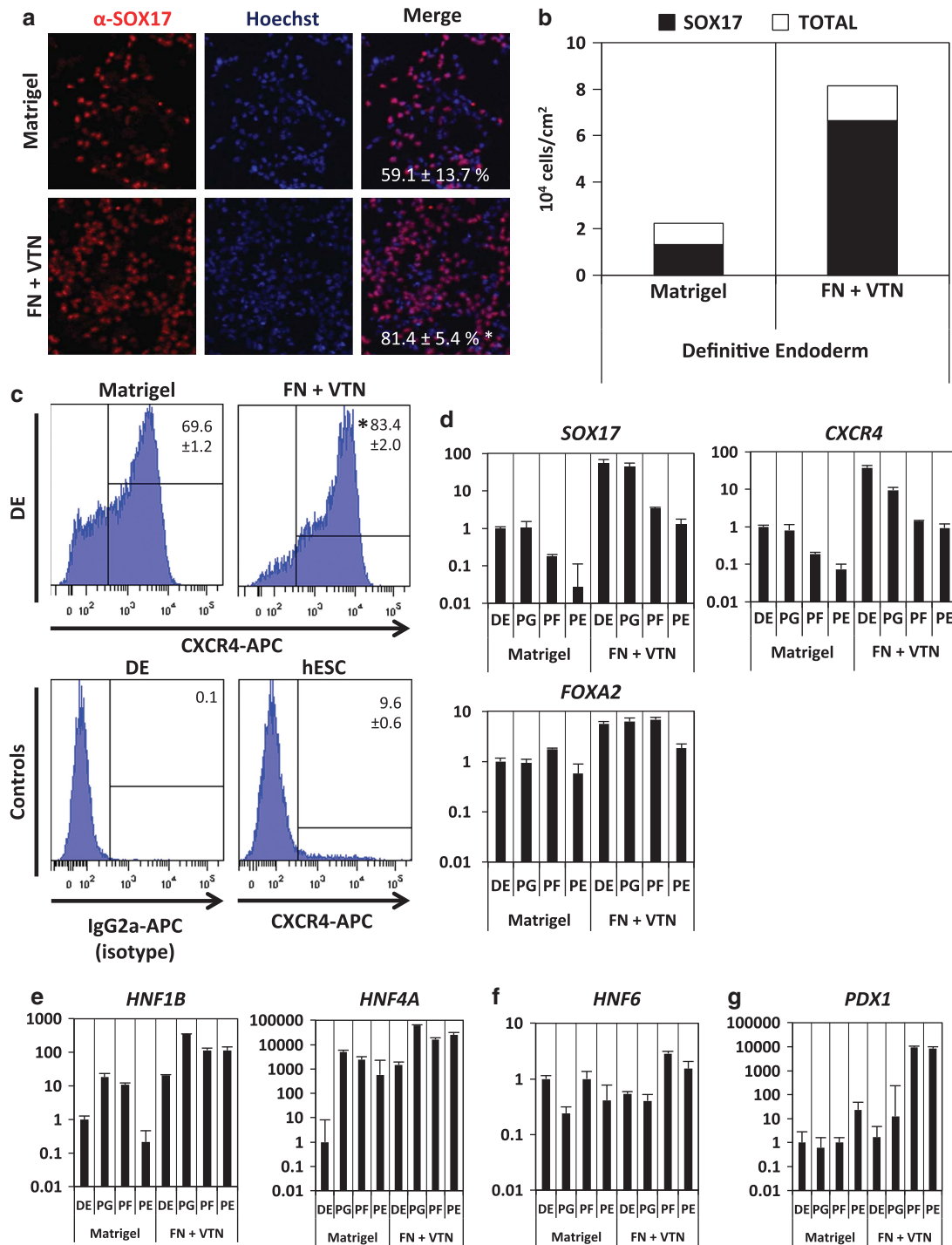


Figure 2 ECMPs improve efficiency of hESC differentiation to DE, PGT, PF endoderm, and PE. HESCs were cultured on MGEL and FN and VTN (FN + VTN) using previously published protocols.^{2,8,9} (a) Representative images of α SOX17 immunofluorescence of HUES9 hESCs differentiated to DE on MGEL and FN + VTN (mean \pm S.E.M.). (b) Quantification of HUES9 hESCs stained by SOX17 cells out of total cell number ($n=3$; mean \pm S.E.M.). (c) Flow cytometric analysis of CXCR4 expression of HUES9 hESCs differentiated to DE on MGEL and FN and VTN (FN + VTN). Gene expression analysis for markers of (d) DE (SOX17, FOXA2, CXCR4), (e) PGT (HNF1 β , HNF4 α), and (f and g) PF and PE (HNF6, PDX1) of HUES9 hESCs differentiated to DE, PGT, PF, and PE on MGEL and FN + VTN. ($n=3$; error bars, S.E.M.). Asterisks indicate statistical significance relative to MGEL as determined by a two tail *t*-test

of DE differentiation over that observed when hESCs were differentiated on either ECMP alone (FN, VTN) or on MGEL (Supplementary Figures 3c and d).

To address whether culture on FN + VTN improved differentiation of hESC to more mature endodermal lineages, HUES9 were cultured on FN + VTN and MGEL and

differentiated to primitive gut tube (PGT), posterior foregut (PF), and pancreatic endoderm (PE) using previously published protocols (Figure 1a).⁹ Expression of *HNF1β* and *HNF4α*, markers of both pancreas and liver development, was higher in cells differentiated on FN + VTN compared with those differentiated on MGEL (Figure 2e). Expression of the PF marker *HNF6* (Figure 2f) and the PE marker *PDX1* (Figure 2g) was higher in FN + VTN *versus* MGEL cultures. These results demonstrate that culture on FN + VTN increases differentiation efficiency toward endodermal lineages.

Integrin expression in hESC differentiation. Having established that FN and VTN were critical ECMP components to promote DE differentiation, we studied the role of integrin receptors in hESC differentiation. HESCs were differentiated to the three germ layers—endoderm, mesoderm, and ectoderm—using previously established protocols^{2,15,16} and analyzed for integrin gene expression. Hierarchical clustering of integrin gene expression revealed specific integrin ‘signatures’ that defined each differentiated cell population, with a set of integrin genes (*ITGA4*, *ITGA5* (integrin $\alpha 5$), *ITGA7*, *ITGAV* (integrin αV), *ITGB2*, *ITGB5*) being upregulated in cells expressing endodermal markers (*SOX17*, *FOXA2*, *CXCR4*) relative to cells expressing either mesodermal (*SMA*, *ACTC1*) or ectodermal (*SOX1*, *SOX2*) marker genes (Figure 3a). Importantly, among these integrins, *ITGA4*, *ITGA5*, *ITGAV*, and *ITGB5* encode subunits of heterodimeric integrin receptors that bind FN and VTN.^{17–21}

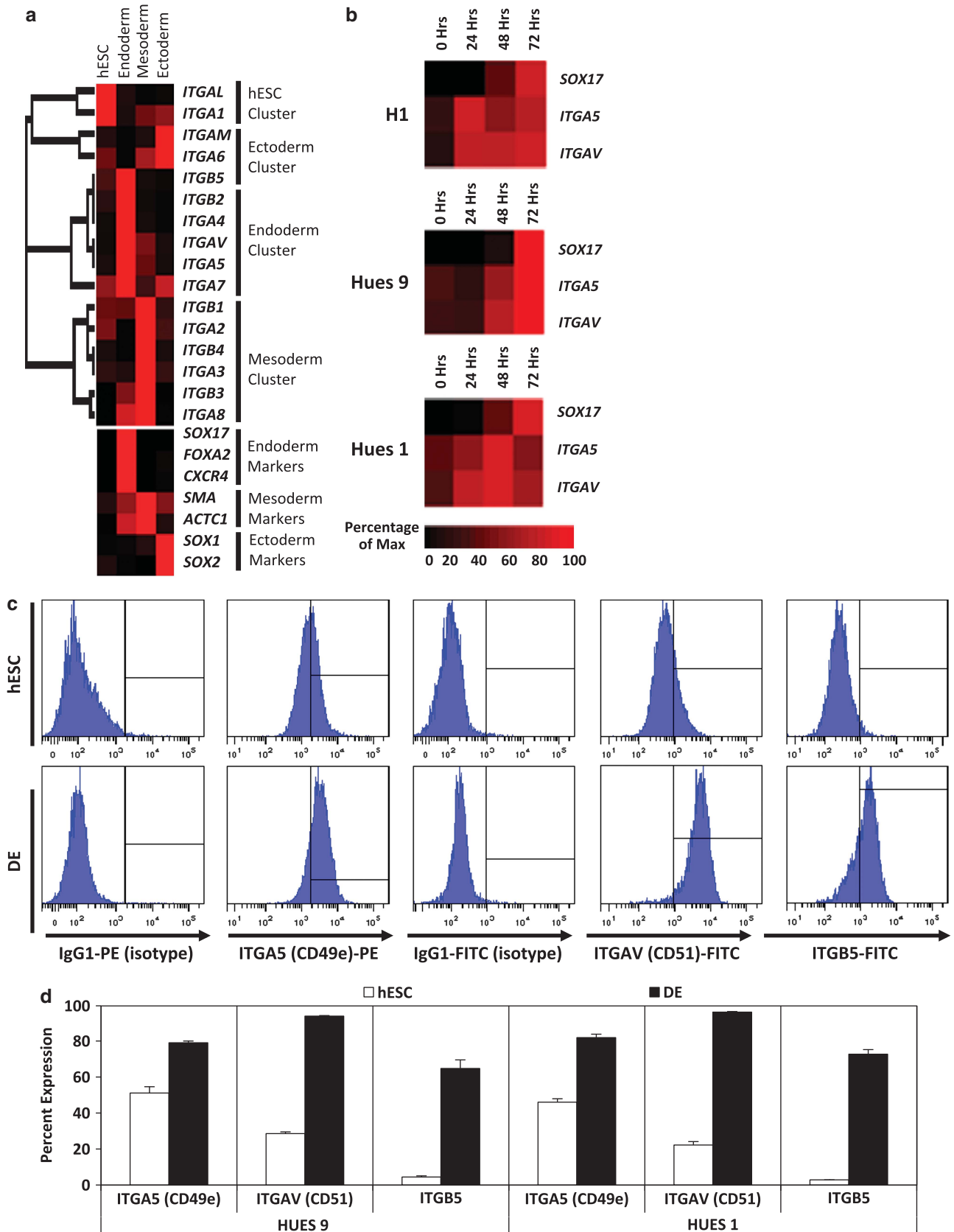
As *ITGA5* is required for hESC binding to FN and *ITGAV*, and *ITGB5* are required for binding to VTN,²² we investigated the expression levels of these integrin subunits as hESCs differentiate to DE. A time course of hESCs differentiating to DE revealed that *ITGA5* and *ITGAV* expression is upregulated in a dynamically similar manner to that of *SOX17* (Figure 3b). Furthermore, expression of *ITGB5* is also upregulated as cells differentiate to DE (Figure 3c), suggesting that hESCs display functional FN and VTN receptors as they differentiate to DE. By contrast, expression of the gene encoding subunits of the LN receptor, *ITGA6*, is significantly downregulated during endoderm differentiation of (Supplementary Figure 4a).

Using flow cytometry, we confirmed that expression of these three integrin receptors, detected by antibodies that bind *ITGA5* (CD49e), *ITGAV* (CD51), and *ITGB5*, is increased in DE *versus* undifferentiated hESCs (Figures 3c and d). In comparison, flow cytometry of *ITGA6* and *ITGB1*, integrin subunits that comprise the LN receptor, were either downregulated or unchanged as hESCs differentiated to DE (Supplementary Figures 4b and c). Taken together, these results suggest that hESCs differentiating to DE significantly upregulate cell surface expression of the subunits that comprise the integrin receptors that bind FN and VTN, the two ECMP components that we identified in our cellular microarray screen to promote DE differentiation.

Knockdown of *ITGA5* and *ITGAV* impairs endoderm formation. To determine to what extent expression of the FN and VTN integrin receptors is functionally important during endodermal differentiation, we used a short hairpin RNA (shRNA) approach to knockdown expression of either

ITGA5 or *ITGAV*. HESCs stably harboring doxycycline (DOX) inducible shRNAs (Figure 4a) to either gene—referred to as *ITGA5*^{shRNA} or *ITGAV*^{shRNA} hESCs—were treated for 3 days with DOX (1 μ g/ml) before induction of endodermal differentiation (see flowchart in Figure 4b). DOX treatment of either *ITGA5*^{shRNA} or *ITGAV*^{shRNA} hESCs and DE led to a significant increase in expression of red fluorescent protein (Supplementary Figure 5a), the expression of which was driven from the same DOX-inducible promoter as the shRNAs. QPCR analysis confirmed that expression of *ITGA5* and *ITGAV* was significantly decreased in DOX-treated undifferentiated hESC and DE cell populations (Figures 4c and d). Flow cytometry revealed that cell surface protein expression of *ITGA5* and *ITGAV* was decreased in DOX-treated DE cell populations (Figures 4e and f). We confirmed that DOX treatment of *ITGA5*^{shRNA} hESCs had no effect on *ITGAV* gene (Supplementary Figure 5b) or cell surface protein expression (Figure 4e). Similarly, DOX treatment of *ITGAV*^{shRNA} hESCs had no effect on *ITGA5* gene (Supplementary Figure 5c) or cell surface protein expression (Figure 4f). Additionally, DOX treatment alone was not responsible for decreases in integrin expression as DOX treatment of wild-type hESCs had no effect on *ITGA5* or *ITGAV* expression (Supplementary Figure 5d). Importantly, expression of the endodermal marker genes, *SOX17*, *FOXA2*, and *CXCR4*, was significantly decreased in hESC-derived DE in which *ITGA5* or *ITGAV* expression was knocked-down by the shRNAs (Figures 4c and d). Furthermore, flow cytometry revealed that *CXCR4* cell surface expression was almost absent in DOX-treated DE cells (Figures 4e and f). IF analysis demonstrated that knockdown of either *ITGA5* or *ITGAV* resulted in a significant reduction in *SOX17* or *FOXA2* staining at DE (Figures 4g and h). These results suggest that expression of FN and VTN integrin receptors *ITGA5* and *ITGAV* is necessary for differentiation of hESCs to DE.

***ITGA5* and *ITGAV* as cell surface markers for the isolation of endodermal progeny from differentiating hESCs.** As increases in *ITGA5* (CD49e) and *ITGAV* (CD51) expression correlate with endodermal differentiation, we tested whether cell separation by flow cytometry for these integrin receptors could be employed to isolate cells with endodermal gene expression signatures (Figure 5a). HESC-derived DE was sorted for *ITGA5* (CD49e) and *ITGAV* (CD51) (Figure 5b) and analyzed for expression of *SOX17* (Figure 5c and Supplementary Figure 6). This analysis revealed that double-positive *ITGA5*(CD49e)⁺/*ITGAV*(CD51)⁺ cells expressed higher amounts of the DE maker gene *SOX17* than single-positive *ITGA5*(CD49e)⁺/*ITGAV*(CD51)⁻ or *ITGA5*(CD49e)⁻/*ITGAV*(CD51)⁺ cells or double-negative *ITGA5*(CD49e)⁻/*ITGAV*(CD51)⁻ cells (Supplementary Figure 6). Furthermore, expression of additional DE marker genes *FOXA2* and *CXCR4* was increased in double-positive cells compared with double-negative cells (Figure 5c). We next investigated if double-positive *ITGA5*(CD49e)⁺/*ITGAV*(CD51)⁺ were capable of differentiating into more mature endodermal progeny. Double-positive *ITGA5*(CD49e)⁺/*ITGAV*(CD51)⁺ and double-negative *ITGA5*(CD49e)⁻/*ITGAV*(CD51)⁻ cells were replated



after cell sorting and differentiated to PGT. Subsequent gene expression analysis revealed that expression of *HNF1 β* and *HNF4 α* , markers of pancreas and liver development, were enriched in the *ITGA5*(CD49e)⁺/*ITGAV*(CD51)⁺ population relative to the *ITGA5*(CD49e)⁻/*ITGAV*(CD51)⁻ population (Figure 5d). Therefore, cell enrichment strategies for *ITGA5* (CD49e) and *ITGAV* (CD51) significantly increase the yield of cells with DE gene expression patterns from differentiating hESC cultures.

Remodeling of the extracellular matrix during endodermal differentiation. In addition to exploring the effects of exogenous ECMP on DE formation, we wanted to investigate the role of endogenous ECMP production and remodeling during endodermal differentiation. To that end, we measured endogenous *ECMP* gene expression of hESCs differentiated to DE (Figure 6a). In general, expression of endogenous ECMPs increased as cells differentiated to DE on MGEL and FN + VTN substrates. Specifically, we observed a statistically significant increased expression of several COLs (*COL4A2*, *COL5A1*, *COL6A1*, *COL7A1*, *COL8A1*, *COL11A1*, *COL12A1*), *FN1*, *VTN*, and LN subunits (*LAMA3*, *LAMAB1*, *LAMAB3*) as hESCs differentiated to DE.

Previous studies have shown ECMP degradation and proteolysis have a critical role in endoderm development and cell differentiation.^{23,24} Therefore, we wanted to determine if ECM remodeling and degradation through the action of matrix metalloproteinases (MMPs) was required for differentiation of hESCs to DE. While expression of *MMP* 1, 3, 7, 10, 12, or 13 was not detected in hESCs or DE (data not shown), we observed a statistically significant increased expression of *MMP* 2, 8, 9, 14, and 15 during DE differentiation (Figure 6b). To test whether MMP activity was required for DE differentiation, we treated cells with broad-spectrum small molecule inhibitors of MMP (Baritasmal, Marimastat, CP471474) and the glycoprotein tissue inhibitor of metalloproteinases (TIMP1) during DE differentiation. Gene expression analysis of DE markers *SOX17*, *FOXA2*, and *CXCR4* revealed that MMP inhibition does not inhibit formation of DE (Figure 6c). Therefore, even though we observe changes in the composition of the extracellular environment during DE differentiation, including endogenous deposition of ECMPs and secretion of MMPs, pharmacological inhibition of MMPs does not appear to disrupt endodermal differentiation of hESCs.

Discussion

The selection of the appropriate extracellular matrix is critical for hESC self-renewal and proliferation,^{13,22} and here we

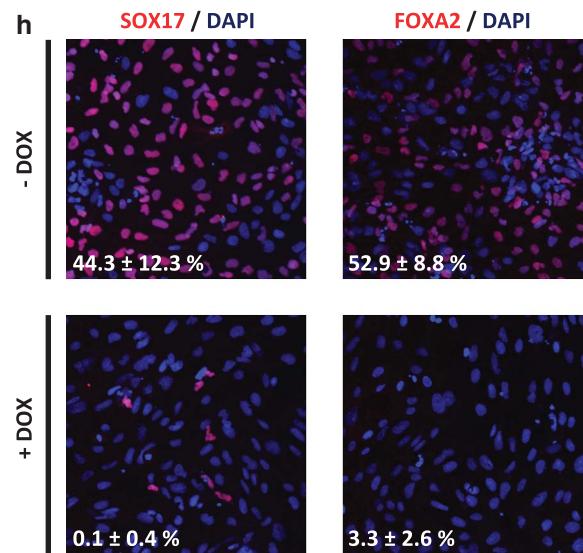
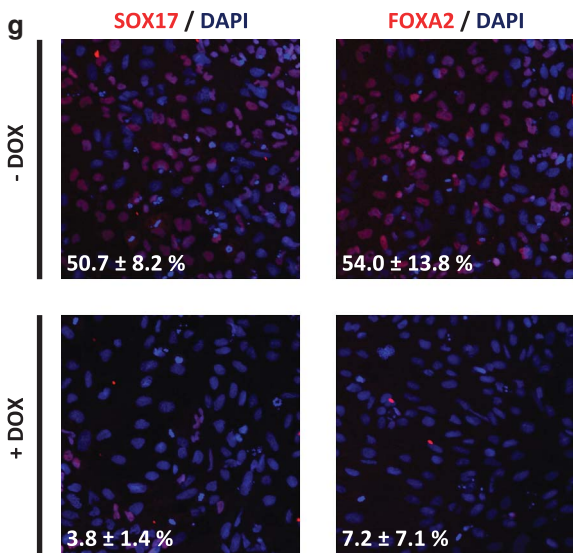
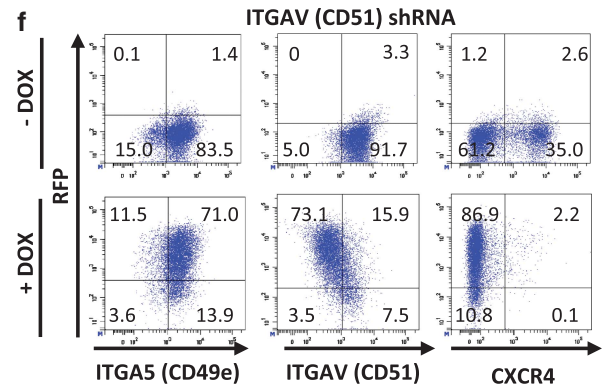
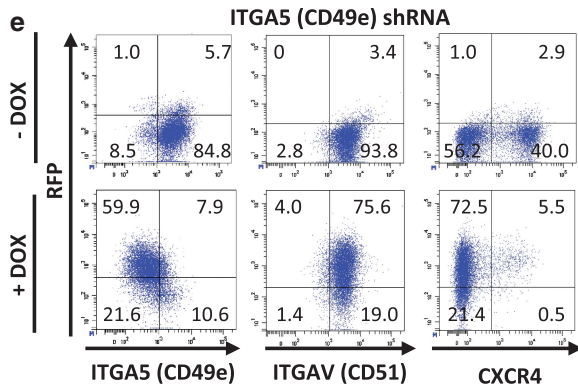
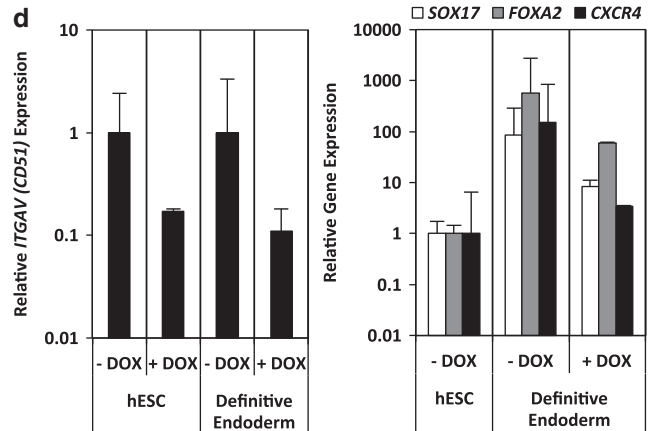
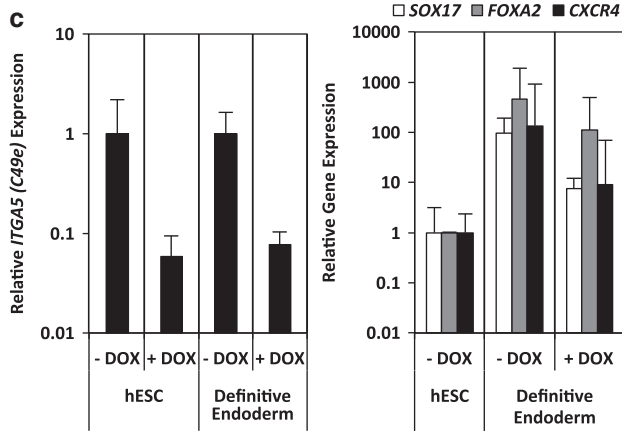
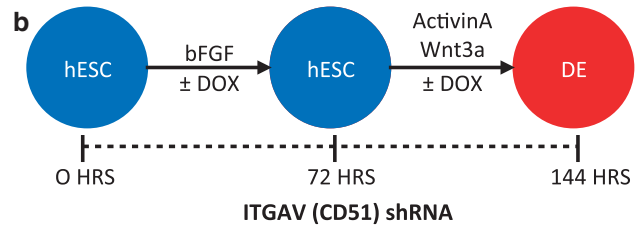
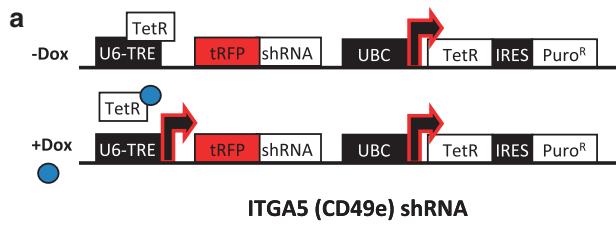
show that the ECMP composition also potentially influences hESC differentiation to DE. By systematically screening hundreds of ECMP combinations, we identified two ECMPs, FN, and VTN, which significantly improve the efficiency of hESC differentiation to DE, thereby overcoming the need for poorly defined and non-human biological components, such as MGEL, in the manipulation of hESCs.

While certain studies have explored the role of physical properties of the microenvironment, including three-dimensional culture²⁵ and substrate rigidity,²⁶ we focused our analysis on the role of the ECM in differentiation and found that changes in the composition of the ECM profoundly affected the differentiation of hESCs to endoderm. It is particularly important to note that the effects of the growth factors inducing DE (*Wnt3a* and *Activin A*) are significantly influenced by ECMP composition. Our results suggest that appropriately defining the ECMP substrate in addition to the soluble signaling molecule environment is critical for improving the differentiation of hESCs to specific lineages.

The differentiation of hESCs to DE resembles that of primitive streak formation and gastrulation where cells invaginate and generate mesendodermal cell populations. These movements of epiblast cells require several growth factor signaling pathways, as well as an ECM. In this process the ECM does not merely function as a scaffold through which cells migrate. Rather, as determined by computational and optical methods, migrating cells move in concert with the ECM with little cellular movement relative to the ECM.²⁷ This study supports the notion that the ECM has a more active role in development than previously appreciated and further underscores the importance of performing screens to identify optimal ECM compositions that promote specific developmental processes.

Consistent with our identification of FN and VTN as critical components that promote endodermal differentiation in cell culture, several studies in model organisms have provided compelling evidence that these ECM components are critical constituents of the microenvironment guiding the processes of primitive streak formation and gastrulation. For example, injection of agents that disrupt integrin-FN interactions, such as RGDS peptides or antibodies and Fab' fragments directed against FN, into chick embryos perturb gastrulation movements.²⁸ Such microinjection experiments in frog embryos have led to similar observations.²⁹ Mice lacking FN-binding integrins die early in development and fail to extend the anterior-posterior axis.³⁰⁻³² Earlier defects, such as during gastrulation, are likely not uncovered due to rescue by maternally contributed FN message and protein. Together, countless studies in a variety of model organisms support the concept that the ECM, and specifically FN, has an

Figure 3 Expression of integrin genes in hESC differentiation. (a) HUES9 hESCs were differentiated *in vitro* to the three germ layers (ectoderm, endoderm, and mesoderm) as previously described.^{2,15,16} QPCR analysis of integrin gene expression was performed. The data is displayed as a heat map where black corresponds to minimum expression levels and red corresponds to maximum levels. Hierarchical clustering of integrin gene expression resulted in segregation of integrins into four groups based on their expression levels in hESCs or germ layer-specific cell types. (b) Time course of DE marker *SOX17* and FN/VTN specific subunits *ITGA5* (CD49e) and *ITGAV* (CD51) gene expression during hESC (H1, HUES1, and HUES9) differentiation to DE. This analysis reveals that *SOX17*, *ITGA5* (CD49e), and *ITGAV* (CD51) gene expression increase in a dynamically similar manner. (c) Representative flow cytometry histograms of cell surface protein expression of FN/VTN specific subunits *ITGA5* (CD49e), *ITGAV* (CD51), and *ITGB5* in hESCs and DE. (d) Quantification of percentage of cell surface protein expression of *ITGA5*⁺ (CD49e⁺), *ITGAV*⁺ (CD51⁺), and *ITGB5*⁺ hESCs and DE (HUES9 and HUES1; n = 3; error bars, S.E.M.)



important and instructive function in early embryogenesis. However, it should be stressed that in our studies only the initial matrix compositions are specified. Cells exposed to these ECMPs remodel the underlying matrix and begin secreting their own ECMPs. Even so, the observed cellular responses are a result of their exposure to the initial composition of the ECM.

Previous studies demonstrated that undifferentiated hESCs express a variety of integrins, including integrins $\alpha 1$, 2, 3, 5, 6, 7, 11, E, and V, and $\beta 1$, 2, 3, and 5.^{33–35} We extended these studies by examining integrin gene expression in undifferentiated hESCs and hESC differentiated to each of the three primitive germ layers—endoderm, mesoderm, and ectoderm. This analysis revealed a specific integrin ‘signature’ that was unique to each of these cell populations. Specifically, we found that *ITGA5* and *ITGAV* gene expression was highly upregulated and *ITGA6* expression was significantly down-regulated in the endodermal lineage. Treatment with specific integrin blocking antibodies revealed that blocking ITGA5 impaired adhesion to FN, blocking ITGAV and ITGB5 reduced the binding to VTN, and blocking ITGA6 inhibited binding to LN.²² Furthermore, ITGA6 binding to LN has been implicated as having a critical role in the self-renewal and maintenance of pluripotent hESCs.³⁶ In this study, we implemented an inducible shRNA system to demonstrate that knockdown of ITGA5 and ITGAV impaired endoderm formation. During development, integrin switching, rapid changes in the proportions of specific integrin subunits expressed at the cell surface, has been implicated as a mechanism that regulates cell differentiation.^{37,38} Together our results suggest a possible mechanism in which hESCs differentiating to DE undergo an integrin switch from an ITGA6 signature which favors binding LN, and thereby maintenance of pluripotency, to an ITGA5 and ITGAV signature, which allows for interaction with FN and VTN and subsequent differentiation to DE.

Mouse models have been used extensively to interrogate integrin expression and functionality during embryonic development.^{37,39,40} Interestingly, mouse embryos stained for different integrin subunits at E6.5 revealed that *Itga5* expression was mainly restricted to endoderm,⁴¹ which is consistent with the ITGA5 expression patterns that we identified in hESC-derived DE. Furthermore, *Itga5* and *ItgaV* are widely expressed during development of many organs of endodermal origin, such as the pancreas, liver, and lungs.^{42–44} Knockout of *Itga5* or *ItgaV* resulted in embryonic lethality,^{32,45} while tissue specific deletion of *Itga5* or *ItgaV* resulted in vasculature and neuronal defects.^{18,32,45,46} Therefore, the novel findings presented here, which demonstrate knockdown of ITGA5 and ITGAV in hESCs impaired endoderm formation in hESCs, suggests that similar integrin knockdown strategies

in hESCs can be used to interrogate the function of various integrin-ECMP interactions during the earliest stages of human development.

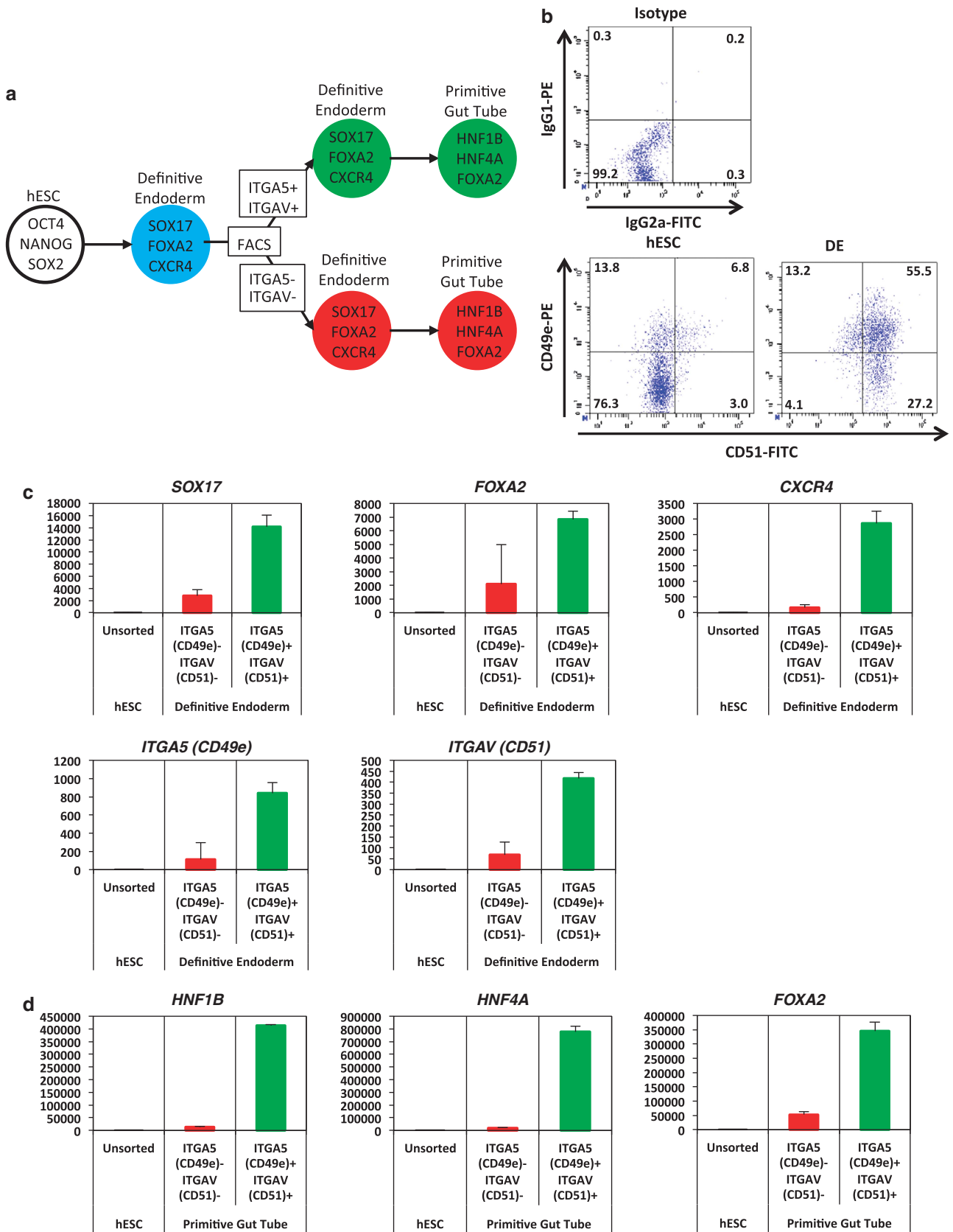
Current hESC differentiation protocols are insufficient in creating pure cell populations, which are required for understanding human development and creating disease relevant models. Therefore, developing sorting strategies for flow cytometry-based isolation of highly pure populations of cells from differentiating hESC cultures is of particular interest.^{47–50} By investigating the role of integrin-ECMP interactions in hESC differentiation to DE, we identified a panel of novel surface integrins, ITGA5 (CD49e) and ITGAV (CD51), that allow for the FACS-based isolation of endodermal cells. In the future, similar integrin ‘signatures’ could be developed that would permit the isolation of lineage committed cells from mixed differentiated hESC cultures.

Materials and Methods

Arrayed cellular microenvironment fabrication. Arrayed cellular microenvironment (ACME) slides were fabricated as previously described. Briefly, glass slides were cleaned, silanized, and then functionalized with a polyacrylamide gel layer. Stock solutions of human COL I, COL III, COL IV, COL V, FN, LN (Sigma-Aldrich, St Louis, MO, USA) and VTN (EMD-Millipore, Billerica, MA, USA) were prepared in an ECMP-printing buffer (200 mM acetate, 10 mM EDTA, 40% (v/v) glycerol, and 0.5% (v/v) triton-X-100 in MQH₂O, with pH adjusted to 4.9 using glacial acetic acid). All ECMP combinations were premixed at a constant protein concentration of 250 μ g/ml in polypropylene 384-well plates. SMP 3.0 spotting pins (Telechem Corp., Atlanta, GA, USA) were washed with 90% ethanol. All printings were performed with a SpotArray 24 (Perkin-Elmer, Waltham, MA, USA) at room temperature (RT) with 65% relative humidity. The printing conditions were a 1000-ms inking time and a 250-ms stamping time. To control for variability, each ECMP combination was printed in replicates of five spots. Each spot had a diameter of 150–200 μ m, and neighboring microenvironments were separated by a center-to-center distance of 450 μ m. A single slide carried 6400 spots arranged in sixteen 20 \times 20 matrices so that one slide carried 1280 unique ECMP conditions. Slides were inspected manually under a light microscope for consistent and uniform ECMP deposition. ECMP spotting was characterized using general protein stain (SYPRO Ruby gel stain, Life Technologies, Carlsbad, CA, USA) or protein specific antibodies (Sigma-Aldrich) as previously described. A single slide from each batch of printed arrays was seeded with HEK-293 (2.5 \times 10⁵ cells per slide) to ensure that each ECMP spot supported cell adhesion.

Cells and culture conditions. The following media were used: mouse embryonic fibroblast (MEF) (1 \times high glucose DMEM, 10% fetal bovine serum (FBS), 1% (v/v) L-glutamine penicillin/streptomycin); H9/WA09 hESCs (1 \times DMEM-F12, 20% (v/v) Knockout Serum Replacement, 1% (v/v) non-essential amino acids, 0.5% (v/v) glutamine, 120 μ M 2-mercaptoethanol (Sigma-Aldrich)); HUES1 and nine hESCs (1 \times Knockout DMEM, 10% (v/v) Knockout Serum Replacement, 10% (v/v) human plasmanate (Chapin Healthcare, Anaheim, CA, USA), 1% (v/v) non-essential amino acids, 1% (v/v) penicillin/streptomycin, 1% (v/v) Gluta-MAX, 55 μ M 2-mercaptoethanol (Sigma-Aldrich)). All media components are from Life Technologies unless indicated otherwise. H9, HUES9, and HUES1 hESC lines were maintained on feeder layers of mitotically inactivated MEFs (2 \times 10⁴/cm²; Millipore). All hESC cultures were supplemented with 30 ng/ml bFGF (Life Technologies). MEF-CM was produced by culturing the appropriate

Figure 4 Expression of FN and VTN receptors integrin $\alpha 5$ (ITGA5) and integrin αv (ITGAV) is required for DE formation. (a) DOX-inducible shRNAs targeting ITGA5 (CD49e) and ITGAV (CD51) were introduced into hESCs (HUES9) using lenti-viral gene transduction. HESCs were selected with Puromycin until stable hESC lines were established. (b) ITGA5^{shRNA} and ITGAV^{shRNA} hESCs were treated with DOX for 72 h before induction of endoderm differentiation. QPCR analysis of DOX treated (c) ITGA5^{shRNA} and (d) ITGAV^{shRNA} hESCs revealed that expression of *ITGA5* (CD49e) and *ITGAV* (CD51), respectively, was decreased in both hESCs and DE. Expression of endoderm genes (*SOX17*, *FOXA2*, and *CXCR4*) was also decreased in DOX-treated hESCs ($n = 3$; error bars, S.E.M). Flow cytometric analysis of (e) ITGA5^{shRNA} and (f) ITGAV^{shRNA} hESCs revealed that cell surface protein expression of ITGA5 (CD49e) and ITGAV (CD51), respectively, was decreased in DOX-treated hESCs compared with untreated cells. Analysis also revealed that ITGAV (CD51) and ITGA5 (CD49e) cell surface protein expression was unchanged in DOX-treated ITGA5^{shRNA} and ITGAV^{shRNA} hESCs, respectively. Cell surface protein expression of the endoderm marker *CXCR4* was also decreased in DOX-treated hESCs. Immunofluorescence of DOX treated (g) ITGA5^{shRNA} and (h) ITGAV^{shRNA} hESCs revealed that protein expression of endoderm markers *SOX17* and *FOXA2* decreased during DOX treatment (mean \pm S.E.M)



hESC medium on MEFs for 24 h. Cells were routinely passaged with Acutase (Millipore), washed, and replated at a density $4.25 \times 10^4/\text{cm}^2$.

Endoderm induction on ACME slides. Before their use, slides were soaked in PBS while being exposed to UVC germicidal radiation in a sterile flow hood for 10 min. Before seeding onto the ACME slides, hESCs were cultured for two passages on MGEL (BD) with MEF-CM supplemented with 30 ng/ml bFGF to remove residual feeder cells. HESCs were then acutase-passaged onto the ACME slides (5.0×10^5 cells per slide) and allowed to settle on the spots for 18 h. Array slides were then gently washed twice with RPMI (Life Technologies) to remove cell debris and residual hESC media. The medium was then changed to RPMI supplemented with 1% (v/v) Gluta-MAX and 100 ng/ml recombinant human Activin A (R&D Systems, Minneapolis, MN, USA). Cells were cultured for 3 days, with FBS concentrations at 0% for the first day and 0.2% for the second and third days. Cultures were supplemented with 30 ng/ml purified mouse Wnt3a for the first day.

Endoderm induction on defined ECMPs. H9, HUES9 and HUES1 were cultured on MGEL (BD) with MEF-CM supplemented with 30 ng/ml bFGF for 2 passages to remove residual MEFs. The human ECMP-coated plates were prepared by coating tissue culture plates in the ECMP (diluted in 10 mM acetic acid) overnight, followed by air drying. $10 \mu\text{g}$ of total protein was plated per cm^2 of culture dish surface. Human ECMP-coated plates were used immediately after air drying. HESCs were passaged at a density of 2.5×10^5 cells/ml onto human ECMP or MGEL-coated plates in order to achieve confluency the following day. HESCs were then gently washed twice with RPMI (Life Technologies) to remove cell debris and residual hESC media. The medium was then changed to RPMI supplemented with 1% (v/v) Gluta-MAX and 100 ng/ml recombinant human Activin A (R&D Systems). Cells were cultured for 3 days, with FBS concentrations at 0% for the first day and 0.2% for the second and third days. Cultures were supplemented with 30 ng/ml purified mouse Wnt3a for the first day. For further differentiation to PGT, the medium was changed to RPMI with 0.2% FBS

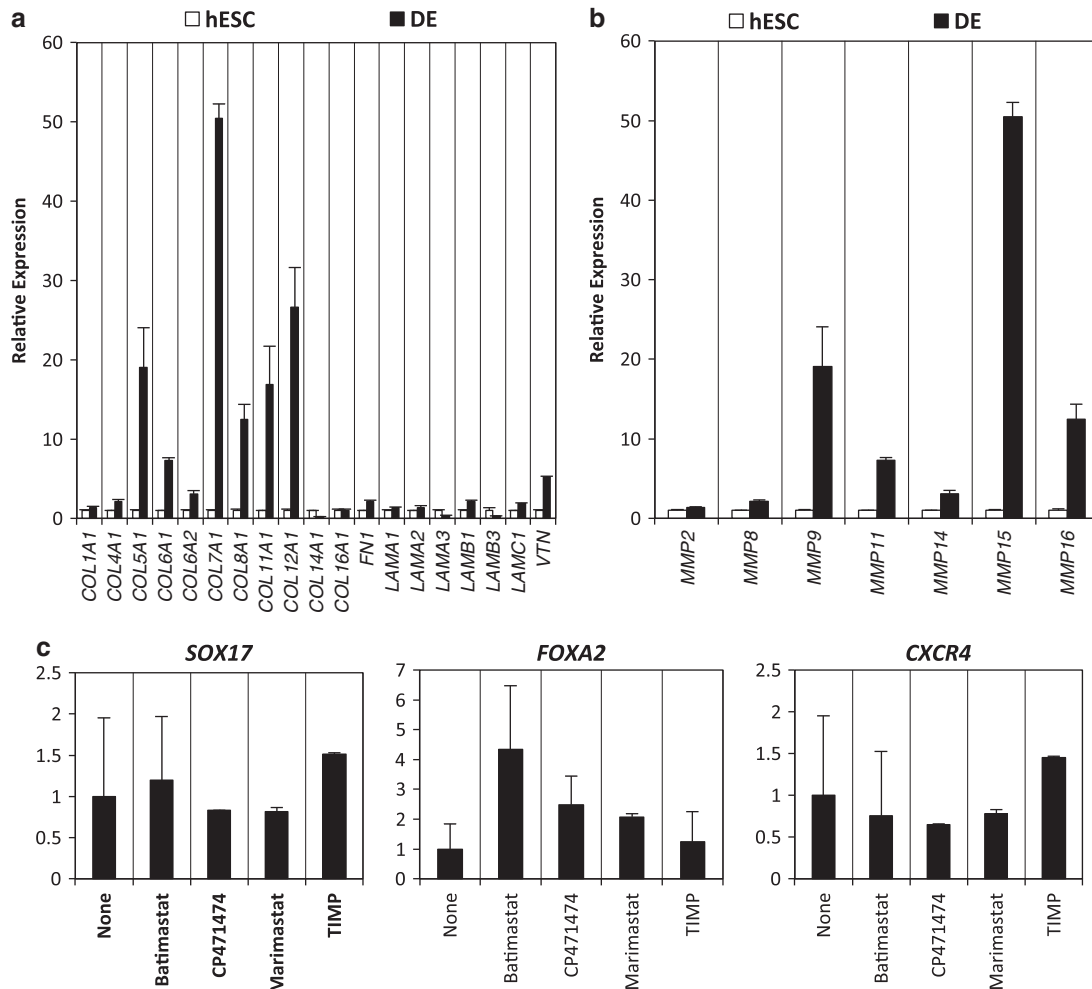


Figure 6 Remodeling of the exogenous extracellular matrix (ECM) during hESC differentiation to DE. QPCR analysis of (a) endogenous ECMP encoding genes and (b) matrix metalloproteinase (MMP) gene expression during hESC differentiation to DE. (c) hESCs were differentiated to DE in the presence of broad-spectrum inhibitors of MMP (Batimastat, Marimastat, and CP471474) and TIMP1. QPCR analysis of DE markers SOX17, FOXA2, and CXCR4 revealed that MMP inhibition had no effect on DE differentiation

Figure 5 Purification of endoderm progeny from differentiating hESCs using the cell surface molecules Integrin $\alpha 5$ (ITGA5/CD49e) and integrin αv (ITGAV/CD51). (a) HESC-differentiated DE cells were sorted based on levels of ITGA5 (CD49e) and ITGAV (CD51) expression. ITGA5 (CD49e)⁺/ITGAV (CD51)⁺ and ITGA5 (CD49e)⁻/ITGAV (CD51)⁻ were replated and further differentiated *in vitro* to PGT cells. (b) Flow cytometry shows that the expression of ITGA5 (CD49e) and ITGAV (CD51) changes during hESC differentiation to DE. (c) HESC-differentiated DE cells were sorted based on levels of ITGA5 (CD49e) and ITGAV (CD51) expression. Gene expression analysis reveals that the expression of endodermal markers SOX17, FOXA2, and CXCR4 were highly enriched in the ITGA5 (CD49e)⁺/ITGAV (CD51)⁺ cells ($n=3$; error bars, S.E.M.). (d) Expression of PGT markers HNF1 β , HNF4 α , and FOXA2 was enriched in *in vitro* differentiated ITGA5 (CD49e)⁺/ITGAV (CD51)⁺ cells ($n=3$; error bars, S.E.M.)

supplemented with 50 ng/ml recombinant human KGF (R&D Systems) for 3 days. For differentiation to PF endoderm, the medium was changed to DMEM with $1 \times$ B27 (Life Technologies), 50 ng/ml recombinant human Noggin (R&D Systems), 0.25 μ M KAAD-cyclopamine (Tocris Biosciences, Bristol, UK), and 2 μ M retinoic acid (Sigma-Aldrich) for 3 days. Finally, for differentiation to PE the medium was changed to DMEM with $1 \times$ B27 (Invitrogen) supplemented with 50 ng/ml recombinant human Noggin, 50 ng/ml recombinant human KGF, and 50 ng/ml recombinant human EGF (R&D Systems) and for 3 days.

Ectoderm and mesoderm differentiation. To differentiate hESCs to ectoderm we modified several previously published protocols.^{9,15,51} To initiate ectoderm differentiation, hPSCs were cultured on MGEL in MEF-CM supplemented with 30 ng/ml FGF2. Cells were then detached with treatment with acutase (Millipore) for 5 min and resuspended in ectoderm embryoid body (EB) media (10% FBS/1% N2/1% B27/DMEM:F12) supplemented with 5 μ M Y-267632 (Stemgent, Cambridge, MA, USA), 50 ng/ml recombinant mouse Noggin (R&D Systems), 0.5 μ M Dorsomorphin (Tocris Biosciences). Next, 7.5×10^5 cells were pipetted to each well of several 6-well ultra low attachment plates (Corning, Lowell, MA, USA). The plates were then placed on an orbital shaker set at 95 r.p.m. in a 37 °C/5% CO₂ tissue culture incubator. The next day, the cells formed spherical clusters and the media was changed to ectoderm EB media without FBS supplemented with 50 ng/ml recombinant mouse Noggin and 0.5 μ M Dorsomorphin. The media was subsequently changed every other day. After 5 days in suspension culture, the EBs were then transferred to a 10-cm dish coated (3×6 wells per 10 cm dish) with growth factor reduced MGEL (1:25 in KnockOut DMEM; BD Biosciences) for attachment. The plated EBs were cultured in ectoderm EB media without FBS supplemented with 50 ng/ml recombinant mouse Noggin and 0.5 μ M Dorsomorphin for an additional 3 days. To differentiate hESC to mesoderm, we modified several previously published protocols.^{16,52} To initiate mesoderm differentiation, hPSCs were cultured on MGEL in MEF-CM supplemented with 30 ng/ml FGF2 until they reached 60% confluency. Cells were then gently washed with RPMI media to remove residual hESC media. The medium was then changed to RPMI supplemented with 0.5% B27 supplement. Cells were cultured for 5 days supplemented with 100 ng/ml recombinant human Activin A (R&D systems) for the first day, and 10 ng/ml BMP4 for days 2–5.

Immunofluorescence. ACME slides and cultures were gently washed twice with staining buffer (PBS w/ 1% (w/v) BSA) before fixation. Cultures were then fixed for 15 min at RT with fresh paraformaldehyde (4% (w/v)). The cultures were washed twice with staining buffer and permeabilized with 0.2% (v/v) triton-X-100 in stain buffer for 20 min at 4 °C. Cultures were then washed twice with staining buffer. Primary antibodies were incubated overnight at 4 °C and then washed twice with stain buffer at RT. Secondary antibodies were incubated at RT for 1 h. Antibodies used are listed in Supplementary Table 2. Nucleic acids were stained for DNA with Hoechst 33342 (2 μ g/ml; Life Technologies) for 5 min at RT. Imaging of was performed using an automated confocal microscope (Olympus Fluoview 1000 (Olympus America, Center Valley, PA, USA) with motorized stage and incubation chamber). Images of ACME slides were quantified using GenePix software (MDS Analytical Technologies, Molecular Devices, Sunnyvale, CA, USA). Quantification of additional images was performed by counting a minimum of nine fields at $\times 20$ magnification.

Flow cytometry and cell replating. Cells were dissociated Acutase (Millipore) for 5 min at 37 °C, triturated, and passed through a 40 μ m cell strainer. Cells were then washed twice with FACS buffer (PBS, 10 mM EDTA, and 2% FBS) and resuspended at a maximum concentration of 5×10^6 cells per 100 μ l. One test volume of antibody was added for each 100 μ l cell suspension (Supplementary Table 2). Cells were stained for 30 min on ice, washed, and resuspended in stain buffer. Cells were analyzed and sorted with a FACSCanto or FACSaria (BD Biosciences). FACS data was analyzed with FACSDiva software (BD Biosciences). For replating experiments, DE cells were stained with CD49e and CD51 and sorted into FACS buffer with 10 nM Y27632 (Stemgent). Sorted cells were replated at a density of 1×10^5 cells/cm² in stage 2 PGT media with 10 nM Y27632 and differentiated for 4 days.

MMP inhibition during endoderm differentiation. Before endoderm differentiation, hESC were treated with 0.5 μ M Batimastat (Tocris Biosciences), 0.5 μ M CP471474 (Tocris Biosciences), 0.5 μ M Marimastat (Tocris Biosciences), or recombinant 130 nM human TIMP1 for 48 h. The medium was then changed to

RPMI supplemented with 1% (v/v) Gluta-MAX and 100 ng/ml recombinant human Activin A (R&D Systems). Cells were cultured for 3 days, with FBS concentrations at 0% for the first day and 0.2% for the second and third days. Cultures were supplemented with 30 ng/ml purified mouse Wnt3a for the first day. MMP inhibition continued throughout the duration of endoderm differentiation.

Quantitative PCR. RNA was isolated from cells using TRIzol (Life Technologies), and treated with DNase I (Life Technologies) to remove traces of DNA. Reverse transcription was performed by means of qScript cDNA Supermix (Quanta Biosciences, Gaithersburg, MA, USA). QPCR was carried out using TaqMan probes (Life Technologies) and TaqMan Fast Universal PCR Master Mix (Life Technologies) on a 7900HT Real Time PCR machine (Life Technologies), with a 10-min gradient to 95 °C followed by 40 cycles at 95 °C for 15 s and 60 °C for 1 min. Taqman gene expression assay primers (Life Technologies; Supplementary Table 3) were used. Gene expression was normalized to 18S rRNA levels. Delta C_t values were calculated as C_t^{target} – C_t^{18S}. All experiments were performed with three technical replicates. Relative fold changes in gene expression were calculated using the 2^{– $\Delta\Delta C_t$} method.⁵³ Data are presented as the average of the biological replicates \pm S.E.M.

Generation of inducible shRNA hESCs. The lenti constructs that were used to generate the inducible shRNA lines were obtained from Open Biosystems (ITGA5:1334333, ITGAV:133468). High titer lenti virus was produced as previously described.^{54,55} HUES9 hESCs were infected overnight with lenti virus and treated with puromycin (0.5 μ g/ml) for 2 weeks.

Statistical analysis. For statistical analysis, unpaired *t*-test were used and a *P*-value < 0.05 was considered statistically significant. All values were presented as mean \pm S.E.M. unless otherwise noted. For each ACME experiment, the ratio (*R*_{*i*}) of the log₂ of the SOX17 signal and the DNA signal was calculated for each spot. From this a differentiation z-score was calculated for each spot $Z_{DIF} = (R_i - \mu_{DIF})/\sigma_{DIF}$, where *R*_{*i*} was the ratio for the spot, μ_{DIF} was the average of the ratios for all spots on each array, and σ_{DIF} was the S.D. of the ratios for all spots on each array. Differentiation z-scores from replication spots (*n* = 5 per ECMP condition) were averaged for each ECMP condition on the array. The replicate average z-scores were displayed in a heat map with rows corresponding to individual ECMP conditions and columns representing independent array experiments. For each array experiment, all columns were mean-centered and normalized to one unit S.D. The rows were clustered using Pearson correlations as a metric of similarity.⁵⁶ All clustering was performed using Gene Cluster.⁵⁶ The results were displayed using a color code with red and green representing an increase and decrease, respectively, relative to the global mean. All heat maps were created using Tree View.⁵⁶ Normalized effect magnitudes were calculated as previously described.¹⁴

Conflict of Interest

The authors declare no conflict of interest.

Acknowledgements. DAB was supported by funding from the UCSD Stem Cell Program and a gift from Michael and Nancy Kaehr. This research was supported in part by the NIDDK Beta Cell Biology Consortium (5U01DK089567-02) and the California Institute for Regenerative Medicine (RB1-01406).

Author contributions

DAB and KW designed the experiments. DAB, CP, and NK performed the experiments. DAB, CP, and KW analyzed the results. DAB and KW wrote the manuscript.

1. Borowiak M, Maehr R, Chen S, Chen AE, Tang W, Fox JL *et al*. Small molecules efficiently direct endodermal differentiation of mouse and human embryonic stem cells. *Cell Stem Cell* 2009; 4: 348–358.
2. D'Amour KA, Agulnick AD, Eliazar S, Kelly OG, Kroon E, Baetge EE. Efficient differentiation of human embryonic stem cells to definitive endoderm. *Nat Biotechnol* 2005; 23: 1534–1541.
3. McLean AB, D'Amour KA, Jones KL, Krishnamoorthy M, Kulik MJ, Reynolds DM *et al*. Activin A efficiently specifies definitive endoderm from human embryonic stem cells only when phosphatidylinositol 3-kinase signaling is suppressed. *Stem Cells* 2007; 25: 29–38.

4. Osafune K, Caron L, Borowiak M, Martinez RJ, Fitz-Gerald CS, Sato Y *et al*. Marked differences in differentiation propensity among human embryonic stem cell lines. *Nat Biotechnol* 2008; **26**: 313–315.
5. Berrier AL, Yamada KM. Cell-matrix adhesion. *J Cell Physiol* 2007; **213**: 565–573.
6. Humphries JD, Byron A, Humphries MJ. Integrin ligands at a glance. *J Cell Sci* 2006; **119**: 3901–3903.
7. Prowse AB, Chong F, Gray PP, Munro TP. Stem cell integrins: implications for *ex-vivo* culture and cellular therapies. *Stem Cell Res* 2011; **6**: 1–12.
8. Kroon E, Martinson LA, Kadoya K, Bang AG, Kelly OG, Eliazar S *et al*. Pancreatic endoderm derived from human embryonic stem cells generates glucose-responsive insulin-secreting cells *in vivo*. *Nat Biotechnol* 2008; **26**: 443–452.
9. Schulz TC, Young HY, Agulnick AD, Babin MJ, Baetge EE, Bang AG *et al*. A scalable system for production of functional pancreatic progenitors from human embryonic stem cells. *PLoS One* 2012; **7**: e37004.
10. Brafman DA, Chang CW, Fernandez A, Willert K, Varghese S, Chien S. Long-term human pluripotent stem cell self-renewal on synthetic polymer surfaces. *Biomaterials* 2010; **31**: 9135–9144.
11. Brafman DA, Chien S, Willert K. Arrayed cellular microenvironments for identifying culture and differentiation conditions for stem, primary and rare cell populations. *Nat Protoc* 2012; **7**: 703–717.
12. Brafman DA, de Minicis S, Seki E, Shah KD, Teng D, Brenner D *et al*. Investigating the role of the extracellular environment in modulating hepatic stellate cell biology with arrayed combinatorial microenvironments. *Integr Biol* 2009; **1**: 513–524.
13. Brafman DA, Shah KD, Fellner T, Chien S, Willert K. Defining long-term maintenance conditions of human embryonic stem cells with arrayed cellular microenvironment technology. *Stem Cells Dev* 2009; **18**: 1141–1154.
14. Box G *et al*. *Statistics for Experimenters*. 1st edn. Wiley: New York, 1978.
15. Chambers SM, Fasano CA, Papapetrou EP, Tomishima M, Sadelain M, Studer L. Highly efficient neural conversion of human ES and iPS cells by dual inhibition of SMAD signaling. *Nat Biotechnol* 2009; **27**: 275–280.
16. Yang L, Soonpaa MH, Adler ED, Roepke TK, Kattman SJ, Kennedy M *et al*. Human cardiovascular progenitor cells develop from a KDR+ embryonic-stem-cell-derived population. *Nature* 2008; **453**: 524–528.
17. Huang X, Griffiths M, Wu J, Farese RV Jr, Sheppard D. Normal development, wound healing, and adenovirus susceptibility in beta5-deficient mice. *Mol Cell Biol* 2000; **20**: 755–759.
18. McCarty JH, Lacy-Hulbert A, Charest A, Bronson RT, Crowley D, Housman D *et al*. Selective ablation of alphaV integrins in the central nervous system leads to cerebral hemorrhage, seizures, axonal degeneration and premature death. *Development* 2005; **132**: 165–176.
19. Munger JS, Huang X, Kawakatsu H, Griffiths MJ, Dalton SL, Wu J *et al*. The integrin alpha V beta 6 binds and activates latent TGF beta 1: a mechanism for regulating pulmonary inflammation and fibrosis. *Cell* 1999; **96**: 319–328.
20. Yang JT, Hynes RO. Fibronectin receptor functions in embryonic cells deficient in alpha 5 beta 1 integrin can be replaced by alpha V integrins. *Mol Biol Cell* 1996; **7**: 1737–1748.
21. Yang JT, Rayburn H, Hynes RO. Cell adhesion events mediated by alpha 4 integrins are essential in placental and cardiac development. *Development* 1995; **121**: 549–560.
22. Braam SR, Zeinstra L, Litjens S, Ward-van Oostwaard D, van den Brink S, van Laake L *et al*. Recombinant vitronectin is a functionally defined substrate that supports human embryonic stem cell self-renewal via alphaVbeta5 integrin. *Stem Cells* 2008; **26**: 2257–2265.
23. Behrendtsen O, Alexander CM, Werb Z. Cooperative interactions between extracellular matrix, integrins and parathyroid hormone-related peptide regulate parietal endoderm differentiation in mouse embryos. *Development* 1995; **121**: 4137–4148.
24. Behrendtsen O, Werb Z. Metalloproteinases regulate parietal endoderm differentiating and migrating in cultured mouse embryos. *Dev Dyn* 1997; **208**: 255–265.
25. Chen SS, Fitzgerald W, Zimmerberg J, Kleinman HK, Margolis L. Cell-cell and cell-extracellular matrix interactions regulate embryonic stem cell differentiation. *Stem Cells* 2007; **25**: 553–561.
26. Engler AJ, Sen S, Sweeney HL, Discher DE. Matrix elasticity directs stem cell lineage specification. *Cell* 2006; **126**: 677–689.
27. Zamir EA, Rongish BJ, Little CD. The ECM moves during primitive streak formation – computation of ECM versus cellular motion. *PLoS Biol* 2008; **6**: e247.
28. Brown AJ, Sanders EJ. Interactions between mesoderm cells and the extracellular matrix following gastrulation in the chick embryo. *J Cell Sci* 1991; **99**(Part 2): 431–441.
29. Boucaut JC, Darribere T, Li SD, Boulekache H, Yamada KM, Thiery JP *et al*. Evidence for the role of fibronectin in amphibian gastrulation. *J Embryol Exp Morphol* 1985; **89**(Suppl): 211–227.
30. George EL, Georges-Labouesse EN, Patel-King RS, Rayburn H, Hynes RO. Defects in mesoderm, neural tube and vascular development in mouse embryos lacking fibronectin. *Development* 1993; **119**: 1079–1091.
31. Takahashi S, Leiss M, Moser M, Ohashi T, Kitao T, Heckmann D *et al*. The RGD motif in fibronectin is essential for development but dispensable for fibril assembly. *J Cell Biol* 2007; **178**: 167–178.
32. Yang JT, Rayburn H, Hynes RO. Embryonic mesodermal defects in alpha 5 integrin-deficient mice. *Development* 1993; **119**: 1093–1105.
33. Alavi SM, Rodina M, Viveiros AT, Cosson J, Gela D, Boryshpolets S *et al*. Effects of osmolality on sperm morphology, motility and flagellar wave parameters in Northern pike (*Esox lucius* L.). *Theriogenology* 2009; **72**: 32–43.
34. Prowse AB, Doran MR, Cooper-White JJ, Chong F, Munro TP, Fitzpatrick J *et al*. Long term culture of human embryonic stem cells on recombinant vitronectin in ascorbate free media. *Biomaterials* 2010; **31**: 8281–8288.
35. Rowland TJ, Miller LM, Blaschke AJ, Doss EL, Bonham AJ, Hikita ST *et al*. Roles of integrins in human induced pluripotent stem cell growth on Matrigel and vitronectin. *Stem Cells Dev* 2010; **19**: 1231–1240.
36. Xu C *et al*. Feeder-free growth of undifferentiated human embryonic stem cells. *Nat Biotechnol* 2001; **19**: 971–974.
37. Meighan CM, Schwarzbauer JE. Temporal and spatial regulation of integrins during development. *Curr Opin Cell Biol* 2008; **20**: 520–524.
38. Zaidel-Bar R, Geiger B. The switchable integrin adhesome. *J Cell Sci* 2010; **123**: 1385–1388.
39. Bokel C, Brown NH. Integrins in development: moving on, responding to, and sticking to the extracellular matrix. *Dev Cell* 2002; **3**: 311–321.
40. Hynes RO. Integrins: bidirectional, allosteric signaling machines. *Cell* 2002; **110**: 673–687.
41. Liu J, He X, Corbett SA, Lowry SF, Graham AM, Fässler R *et al*. Integrins are required for the differentiation of visceral endoderm. *J Cell Sci* 2009; **122**: 233–242.
42. Coraux C, Delplanque A, Hinnrasky J, Peault B, Puchelle E, Gaillard D. Distribution of integrins during human fetal lung development. *J Histochem Cytochem* 1998; **46**: 803–810.
43. Shiojiri N, Sugiyama Y. Immunolocalization of extracellular matrix components and integrins during mouse liver development. *Hepatology* 2004; **40**: 346–355.
44. Wang R, Li J, Lyte K, Yashpal NK, Fellows F, Goodyer CG. Role for beta1 integrin and its associated alpha3, alpha5, and alpha6 subunits in development of the human fetal pancreas. *Diabetes* 2005; **54**: 2080–2089.
45. van der Flier A, Badu-Nkansah K, Whittaker CA, Crowley D, Bronson RT, Lacy-Hulbert A *et al*. Endothelial alpha5 and alphaV integrins cooperate in remodeling of the vasculature during development. *Development* 2010; **137**: 2439–2449.
46. Marchetti G, Escuin S, van der Flier A, De Arcangelis A, Hynes RO, Georges-Labouesse E *et al*. Integrin alpha5beta1 is necessary for regulation of radial migration of cortical neurons during mouse brain development. *Eur J Neurosci* 2010; **31**: 399–409.
47. Dubois NC, Craft AM, Sharma P, Elliott DA, Stanley EG, Elefanti AG *et al*. SIRPA is a specific cell-surface marker for isolating cardiomyocytes derived from human pluripotent stem cells. *Nat Biotechnol* 2011; **29**: 1011–1018.
48. Elliott DA, Braam SR, Koutsis K, Ng ES, Jenny R, Lagerqvist EL *et al*. NKX2-5(eGFP/w) hESCs for isolation of human cardiac progenitors and cardiomyocytes. *Nat Methods* 2011; **8**: 1037–1040.
49. Wang P, Rodriguez RT, Wang J, Ghodasara A, Kim SK. Targeting SOX17 in human embryonic stem cells creates unique strategies for isolating and analyzing developing endoderm. *Cell Stem Cell* 2011; **8**: 335–346.
50. Yuan SH, Martin J, Eila J, Flippin J, Paramban RI, Hefferan MP *et al*. Cell-surface marker signatures for the isolation of neural stem cells, glia and neurons derived from human pluripotent stem cells. *PLoS One* 2011; **6**: e17540.
51. Watanabe K, Kamiya D, Nishiyama A, Katayama T, Nozaki S, Kawasaki H *et al*. Directed differentiation of telencephalic precursors from embryonic stem cells. *Nat Neurosci* 2005; **8**: 288–296.
52. Laflamme MA, Chen KY, Naumova AV, Muskheli V, Fugate JA, Dupras SK *et al*. Cardiomyocytes derived from human embryonic stem cells in pro-survival factors enhance function of infarcted rat hearts. *Nat Biotechnol* 2007; **25**: 1015–1024.
53. VanGuilder HD, Vrana KE, Freeman WM. Twenty-five years of quantitative PCR for gene expression analysis. *Biotechniques* 2008; **44**: 619–626.
54. Miyoshi H *et al*. Development of a self-inactivating lentivirus vector. *J Virol* 1998; **72**: 8150–8157.
55. Zufferey R, Dull T, Mandel RJ, Bukovsky A, Quiroz D, Naldini L *et al*. Self-inactivating lentivirus vector for safe and efficient *in vivo* gene delivery. *J Virol* 1998; **72**: 9873–9880.
56. Eisen MB, Spellman PT, Brown PO, Botstein D. Cluster analysis and display of genome-wide expression patterns. *Proc Natl Acad Sci USA* 1998; **95**: 14863–14868.



This work is licensed under the Creative Commons Attribution-NonCommercial-No Derivative Works 3.0 Unported License. To view a copy of this license, visit <http://creativecommons.org/licenses/by-nc-nd/3.0/>

Supplementary Information accompanies the paper on Cell Death and Differentiation website (<http://www.nature.com/cdd>)